John von Neumann Institute for Computing

Molecular Dynamics Beyond the Born-Oppenheimer Approximation: Mixed Quantum–Classical Approaches

Nikos L. Doltsinis

published in

Computational Nanoscience: Do It Yourself!,
J. Grotendorst, S. Blügel, D. Marx (Eds.),
John von Neumann Institute for Computing, Jülich,
NIC Series, Vol. **31**, ISBN 3-00-017350-1, pp. 389-409, 2006.

http://www.fz-juelich.de/nic-series/volume31

Molecular Dynamics Beyond the Born-Oppenheimer Approximation: Mixed Quantum–Classical Approaches

Nikos L. Doltsinis

Chair of Theoretical Chemistry
Ruhr-Universität Bochum
44780 Bochum, Germany
E-mail: nikos.doltsinis@theochem.rub.de

This contribution takes a closer look at the foundations of conventional molecular dynamics simulations such as the Born-Oppenheimer approximation and the treatment of atomic nuclei according to the laws of classical mechanics. Regimes of validity of the adiabatic approximation are defined and models that take into account nonadiabatic effects in situations where the Born-Oppenheimer approximation breaks down are introduced. We focus on two mixed quantum-classical methods that differ only in the way the forces on the — classical — atomic nuclei are determined from the solutions to the time-independent electronic Schrödinger equation. In the Ehrenfest approach, the system moves on a single potential energy surface obtained by weighted averaging over all adiabatic states, whereas the 'surface hopping' method allows transitions between pure adiabatic potential energy surfaces according to their weights. In both cases, the weights are the squares of the coefficients of the total electronic wavefunction expanded in terms of the adiabatic state functions.

1 Introduction

Molecular dynamics (MD), in the literal sense, is the simultaneous motion of a number of atomic nuclei and electrons forming a molecular entity. Strictly speaking, a complete description of such a system requires solving the full time-dependent Schrödinger equation including both electronic and nuclear degrees of freedom. This, however, is a formidable computational task which is in fact altogether unfeasible, at present, for systems consisting of more than three atoms and more than one electronic state[1,2]. In order to study the dynamics of the vast majority of chemical systems, several approximations, therefore, have to be imposed.

Firstly, it is assumed in MD that the motions of slow and fast degrees of freedom are separable (adiabatic or Born-Oppenheimer approximation). In the molecular context this means that the electron cloud adjusts instantly to changes in the nuclear configuration. As a consequence, nuclear motion evolves on a *single* potential energy surface (PES), associated with a *single* electronic quantum state, which is obtained by solving the time-independent Schrödinger equation for a series of fixed nuclear geometries. In practice, most MD simulations are performed on a *ground state* PES.

Moreover, in addition to making the Born-Oppenheimer approximation, MD treats the atomic nuclei as *classical* particles whose trajectories are computed by integrating Newton's equations of motion.

MD has been applied with great success to study a wide range of systems from biomolecules to condensed phases[3,4]. Its underlying approximations, on the other hand,

break down in many important physical situations and extensions of the method are needed for those scenarios. An accurate description of hydrogen motion, for instance, requires quantum mechanical treatment. Processes such as charge-transfer reactions and photochemistry are inherently *nonadiabatic*, i.e., they involve (avoided) crossings of different electronic states rendering the Born-Oppenheimer approximation invalid.

Critical assessment of the adiabatic approximation as well as discussion of nonadiabatic extensions will be the subject of the present paper.

Since our focus here is on potential applicability to large-scale systems, we shall retain the classical treatment of the nuclei and only describe the electrons quantum mechanically. We will use the term semiclassical for such mixed quantum-classical models. Both expressions can be frequently found in the literature.

Out of the great many semiclassical approaches to nonadiabatic dynamics that have been proposed two "standard" methods different in philosophy have emerged as the most popular ones. One extreme is the Ehrenfest method[2,5–10], where the nuclei move on *one* effective PES which is an average of all adiabatic states involved weighted by their populations (therefore also called mean-field method). The other extreme is the surface hopping approach[11,12,8,9,13,14], where the nuclei evolve on pure adiabatic PESs, but switches between adiabatic states are allowed when their populations change.

This article is organised as follows. In Section 2, the Born-Oppenheimer approximation is introduced. Starting from the full time-dependent Schrödinger equation, the uncoupled nuclear equations of motion are derived. Section 3 deals with the semiclassical approach replacing the nuclear wavefunction by a classical trajectory. This will form the basis of all nonadiabatic methods presented in later sections. Conditions for the validity of the Born-Oppenheimer approximation are discussed qualitatively. Two of the most commonly employed nonadiabatic dynamics methods are described in Section 4, namely the Ehrenfest and the surface hopping methods. The section closes by presenting a recent implementation of the surface hopping technique within the framework of Car-Parrinello MD[52–54] together with an application to the cis-trans photoisomerisation of formaldimine as a case study[52].

2 Born-Oppenheimer Approximation

A complete, non-relativistic, description of a system of N atoms having the positions $\mathbf{R} = (\mathbf{R}_1, \mathbf{R}_2, \ldots, \mathbf{R}_K, \ldots, \mathbf{R}_N)$ with n electrons located at $\mathbf{r} = (\mathbf{r}_1, \mathbf{r}_2, \ldots, \mathbf{r}_K, \ldots, \mathbf{r}_n)$ is provided by the time-dependent Schrödinger equation

$$\mathcal{H}\Xi(\mathbf{r}, \mathbf{R}; t) = i\hbar \frac{\partial}{\partial t}\Xi(\mathbf{r}, \mathbf{R}; t) \quad , \tag{1}$$

with the total Hamiltonian

$$\mathcal{H}(\mathbf{r}, \mathbf{R}) = \mathcal{T}(\mathbf{R}) + \mathcal{T}(\mathbf{r}) + \mathcal{V}(\mathbf{R}) + \mathcal{V}(\mathbf{r}, \mathbf{R}) + \mathcal{V}(\mathbf{r}) \quad , \tag{2}$$

being the sum of kinetic energy of the atomic nuclei,

$$\mathcal{T}(\mathbf{R}) = -\frac{\hbar^2}{2} \sum_{K=1}^{N} \frac{\boldsymbol{\nabla}_K^2}{M_K} \quad , \tag{3}$$

kinetic energy of the electrons,

$$\mathcal{T}(\mathbf{r}) = -\frac{\hbar^2}{2m_e}\sum_{k=1}^{n}\boldsymbol{\nabla}_k^2 \quad , \tag{4}$$

internuclear repulsion,

$$\mathcal{V}(\mathbf{R}) = \frac{e^2}{4\pi\epsilon_0}\sum_{K=1}^{N-1}\sum_{L>K}^{N}\frac{Z_K Z_L}{|\mathbf{R}_K - \mathbf{R}_L|} \quad , \tag{5}$$

electronic – nuclear attraction,

$$\mathcal{V}(\mathbf{r},\mathbf{R}) = -\frac{e^2}{4\pi\epsilon_0}\sum_{K=1}^{N}\sum_{k=1}^{n}\frac{Z_K}{|\mathbf{r}_k - \mathbf{R}_K|} \quad , \tag{6}$$

and interelectronic repulsion,

$$\mathcal{V}(\mathbf{r}) = \frac{e^2}{4\pi\epsilon_0}\sum_{k=1}^{n-1}\sum_{l>k}^{n}\frac{1}{|\mathbf{r}_k - \mathbf{r}_l|} \quad . \tag{7}$$

Here, M_K and Z_K denote the mass and atomic number of nucleus K; m_e and e are the electronic mass and elementary charge, and ϵ_0 is the permittivity of vacuum. The nabla operators $\boldsymbol{\nabla}_K$ and $\boldsymbol{\nabla}_k$ act on the coordinates of nucleus K and electron k, respectively.

Defining the electronic Hamiltonian (fixed-nuclei approximation of $\mathcal{H}$) as

$$\mathcal{H}_{\text{el}}(\mathbf{r},\mathbf{R}) = \mathcal{T}(\mathbf{r}) + \mathcal{V}(\mathbf{R}) + \mathcal{V}(\mathbf{r},\mathbf{R}) + \mathcal{V}(\mathbf{r}) \quad , \tag{8}$$

we can rewrite the total Hamiltonian as

$$\mathcal{H}(\mathbf{r},\mathbf{R}) = \mathcal{T}(\mathbf{R}) + \mathcal{H}_{\text{el}}(\mathbf{r},\mathbf{R}) \quad . \tag{9}$$

Let us suppose the solutions of the time-independent (electronic) Schrödinger equation,

$$\mathcal{H}_{\text{el}}(\mathbf{r},\mathbf{R})\phi_i(\mathbf{r},\mathbf{R}) = E_i(\mathbf{R})\phi_i(\mathbf{r},\mathbf{R}) \quad , \tag{10}$$

are known. Furthermore, the spectrum of $\mathcal{H}_{\text{el}}(\mathbf{r},\mathbf{R})$ is assumed to be discrete and the eigenfunctions orthonormalised:

$$\int_{-\infty}^{\infty}\phi_i^*(\mathbf{r},\mathbf{R})\phi_j(\mathbf{r},\mathbf{R})\mathrm{d}\mathbf{r} \equiv \langle\phi_i|\phi_j\rangle = \delta_{ij} \quad . \tag{11}$$

The total wavefunction Ξ can be expanded in terms of the eigenfunctions of $\mathcal{H}_{\text{el}}$ since these form a complete set:

$$\Xi(\mathbf{r},\mathbf{R};t) = \sum_j \phi_j(\mathbf{r},\mathbf{R})\chi_j(\mathbf{R},t) \quad . \tag{12}$$

Insertion of this ansatz into the time-dependent Schrödinger equation (1) followed by multiplication from the left by $\phi_i^*(\mathbf{r},\mathbf{R})$ and integration over the electronic coordinates leads to a set of coupled differential equations:

$$\left[\mathcal{T}(\mathbf{R}) + E_i(\mathbf{R})\right]\chi_i + \sum_j \mathcal{C}_{ij}\chi_j = i\hbar\frac{\partial}{\partial t}\chi_i \quad , \tag{13}$$

where the coupling operator $\mathcal{C}_{ij}$ is defined as

$$\mathcal{C}_{ij} \equiv \langle\phi_i|\mathcal{T}(\mathbf{R})|\phi_j\rangle - \sum_K \frac{\hbar^2}{M_K}\langle\phi_i|\boldsymbol{\nabla}_K|\phi_j\rangle\boldsymbol{\nabla}_K \quad . \tag{14}$$

The diagonal term $\mathcal{C}_{ii}$ represents a correction to the (adiabatic) eigenvalue E_i of the electronic Schrödinger equation (10). In the case that all coupling operators $\mathcal{C}_{ij}$ are negligible, the set of differential Eqs. (13) becomes uncoupled:

$$\left[\mathcal{T}(\mathbf{R}) + E_i(\mathbf{R})\right]\chi_i = i\hbar\frac{\partial}{\partial t}\chi_i \quad . \tag{15}$$

This means that the nuclear motion proceeds without changes of the quantum state of the electron cloud and, correspondingly, the wavefunction (Eq. (12)) is reduced to a single term (adiabatic approximation):

$$\Xi(\mathbf{r},\mathbf{R};t) \approx \phi_i(\mathbf{r},\mathbf{R})\chi_i(\mathbf{R},t) \quad . \tag{16}$$

For a great number of physical situations the Born-Oppenheimer approximation can be safely applied. On the other hand, there are many important chemical phenomena like, for instance, charge transfer and photoisomerisation reactions, whose very existence is due to the inseparability of electronic and nuclear motion. Inclusion of nonadiabatic effects will be the subject of the following sections.

3 Mixed Quantum–Classical Approach

Further simplification of the problem can be achieved by describing nuclear motion by classical mechanics and only the electrons quantum mechanically. In this so-called mixed quantum–classical (sometimes referred to as semiclassical) approach[15,16], the atomic nuclei follow some trajectory $\mathbf{R}(t)$ while the electronic motion is captured by some time-dependent total wavefunction $\Phi(\mathbf{r};t)$ satisfying the time-dependent electronic Schrödinger equation,

$$\mathcal{H}_{\text{el}}(\mathbf{r},\mathbf{R}(t))\Phi(\mathbf{r};t) = i\hbar\frac{\partial}{\partial t}\Phi(\mathbf{r};t) \quad . \tag{17}$$

Again, the total wavefunction is written as a linear combination of adiabatic eigenfunctions $\phi_i(\mathbf{r},\mathbf{R})$ (solutions of the time-independent Schrödinger equation (10)):

$$\Phi(\mathbf{r};t) = \sum_j a_j(t)\phi_j(\mathbf{r},\mathbf{R})e^{-\frac{i}{\hbar}\int E_j(\mathbf{R})\mathrm{d}t} \quad . \tag{18}$$

Insertion of this ansatz into the time-dependent electronic Schrödinger equation (17) followed by multiplication from the left by $\phi_i^*(\mathbf{r},\mathbf{R})$ and integration over the electronic coordinates leads to a set of coupled differential equations:

$$\dot{a}_i = -\sum_j a_j C_{ij} e^{-\frac{i}{\hbar}\int(E_j - E_i)\mathrm{d}t} \quad , \tag{19}$$

where

$$C_{ij} \equiv \langle\phi_i|\frac{\partial}{\partial t}|\phi_j\rangle \tag{20}$$

are the nonadiabatic coupling elements. Integration of Eqs. (19) yields the expansion coefficients $a_i(t)$ whose square modulus, $|a_i(t)|^2$, can be interpreted as the probability of finding the system in the adiabatic state i at time t.

We now want to develop a condition for the validity of the Born-Oppenheimer approximation based on qualitative arguments. For this purpose, we shall consider a two-state system. To illustrate the problem, Figure 1 shows the avoided crossing between the covalent and ionic potential energy curves of NaCl[17,18]. As we can see, the adiabatic wavefunctions ϕ_1 and ϕ_2 change their character as the bond length is varied. The characteristic length, l, over which ϕ_1 and ϕ_2 change significantly clearly depends on the nuclear configuration $\mathbf{R}$; in the vicinity of the NaCl avoided crossing, for instance, the character of the wavefunctions varies rapidly, whereas at large separations it remains more or less constant.

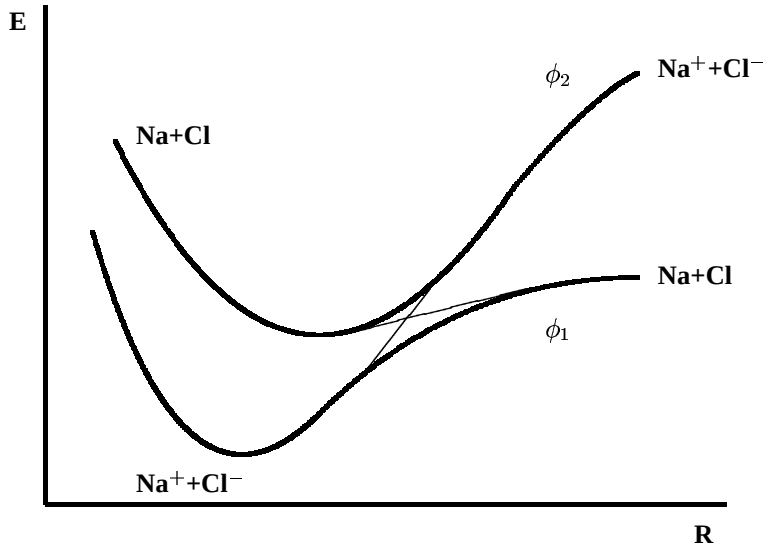

Figure 1. Avoided crossing between the covalent and ionic adiabatic potential curves of NaCl (thin lines: crossing of diabatic states).

Division of the characteristic length l by the velocity of the nuclei, $\dot{R} = |\dot{\mathbf{R}}|$, at a particular configuration $\mathbf{R}$ defines the time the system needs to travel the distance l around $\mathbf{R}$:

$$\text{passage time } \tau_p = \frac{l}{\dot{R}} \quad . \tag{21}$$

In order for the Born-Oppenheimer approximation to be valid, the electron cloud has to adjust instantly to the nuclear changes. The time scale characteristic of electronic motion can be obtained from the relation

$$\Delta E = |E_1 - E_2| = \hbar\omega \tag{22}$$

by taking the inverse transition frequency:

$$\tau_e = \frac{1}{\omega} = \frac{\hbar}{\Delta E} \quad . \tag{23}$$

The ratio

$$\xi = \frac{\tau_p}{\tau_e} = \frac{\Delta E\, l}{\hbar \dot{R}} \tag{24}$$

is the so-called Massay parameter. For values $\xi \gg 1$, i.e. large energy gaps ΔE and small velocities $\dot{R}$, nonadiabatic effects are negligible. In this case, if the system is prepared in some pure adiabatic state i ($|a_i|^2 = 1$) at time $t = 0$, the rhs of Eq. (19) will be zero at all times and the wavefunction expansion (Eq. (18)) can be replaced by a single term:

$$\Phi(\mathbf{r}; t) = \phi_i(\mathbf{r}, \mathbf{R}) e^{-\frac{i}{\hbar} \int E_i(\mathbf{R}) \mathrm{d}t} \quad . \tag{25}$$

The atomic nuclei are then propagated by solving Newton's equations

$$M_K \ddot{\mathbf{R}}_K = \mathbf{F}_K(\mathbf{R}) \quad , \tag{26}$$

where

$$\mathbf{F}_K(\mathbf{R}) = -\boldsymbol{\nabla}_K E_i(\mathbf{R}) \tag{27}$$

is the force on atom K.

4 Approaches to Nonadiabatic Dynamics

4.1 Mean-Field (Ehrenfest) Method

As we have discussed in the previous section, nonadiabaticity involves changes in the adiabatic state populations $|a_i|^2$ with changing nuclear configuration. Clearly, such a distortion of the electron cloud will, in turn, influence the nuclear trajectory. Although there are situations in which the impact of electronic nonadiabaticity on nuclear motion is negligible (e.g. for high energy collisions or small energy separations between adiabatic states), for many chemical systems it is of prime importance to properly incorporate electronic–nuclear feedback[8,9].

The simplest way of doing this is to replace the adiabatic potential energy surface E_i in Eq. (27) by the energy expectation value

$$E^{\text{eff}} = \langle \Phi | \mathcal{H}_{\text{el}} | \Phi \rangle = \sum_i |a_i|^2 E_i \quad , \tag{28}$$

where we have used Eq. (18). Thus, the atoms evolve on an effective potential representing an average over the adiabatic states weighted by their state populations $|a_i|^2$ (as illustrated in Figure 2). The method is therefore referred to as mean-field (also known as Ehrenfest) approach.

It is instructive to derive an expression for the nuclear forces either from the gradient of Eq. (28) or using the Hellmann-Feynman theorem

$$\mathbf{F}_K = -\langle \Phi | \boldsymbol{\nabla}_K \mathcal{H}_{\text{el}} | \Phi \rangle \quad . \tag{29}$$

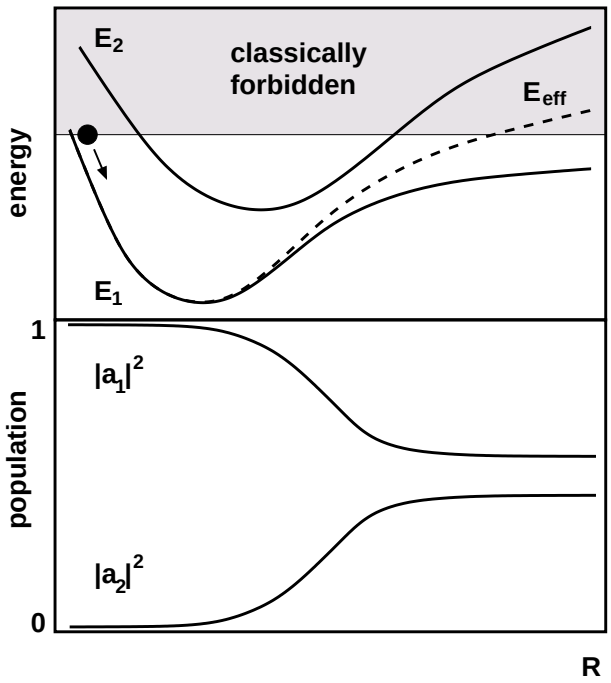

Figure 2. Top: avoided crossing between two adiabatic PES, E_1 and E_2, and effective potential, $E_{\rm eff}$, on which the nuclei are propagated in the Ehrenfest method. In the asymptotic region (right) $E_{\rm eff}$ contains contributions from classically forbidden regions of E_2. Bottom: corresponding adiabatic state populations $|a_1|^2$ and $|a_1|^2$. The system is prepared in state 1 initially with zero kinetic energy. Upon entering the coupling region state 2 is increasingly populated.

Opting for the latter, we start by writing down the relation

$$\begin{aligned} \boldsymbol{\nabla}_K \langle\phi_i|\mathcal{H}_{\rm el}|\phi_j\rangle &= \boldsymbol{\nabla}_K E_i \delta_{ij} && (30)\\ &= \langle\boldsymbol{\nabla}_K\phi_i|\mathcal{H}_{\rm el}|\phi_j\rangle + \langle\phi_i|\boldsymbol{\nabla}_K\mathcal{H}_{\rm el}|\phi_j\rangle + \langle\phi_i|\mathcal{H}_{\rm el}|\boldsymbol{\nabla}_K\phi_j\rangle && (31)\\ &= \langle\phi_i|\boldsymbol{\nabla}_K\mathcal{H}_{\rm el}|\phi_j\rangle + (E_j - E_i)\mathbf{d}_{ji} \quad , && (32) \end{aligned}$$

where we have defined the nonadiabatic coupling vectors, $\mathbf{d}_{ji}$, as

$$\mathbf{d}_{ji} = \langle\phi_j|\boldsymbol{\nabla}_K|\phi_i\rangle \quad , \tag{33}$$

and used Eq. (10) together with the hermiticity of $\mathcal{H}_{\rm el}$:

$$\langle\phi_i|\mathcal{H}_{\rm el}|\boldsymbol{\nabla}_K\phi_j\rangle = \langle\boldsymbol{\nabla}_K\phi_j|\mathcal{H}_{\rm el}|\phi_i\rangle^* = \langle\boldsymbol{\nabla}_K\phi_j|E_j\phi_i\rangle^* = E_i\mathbf{d}_{ij}^* = -E_i\mathbf{d}_{ji} \quad . \tag{34}$$

Note that

$$\mathbf{d}_{ji}^* = -\mathbf{d}_{ij} \quad , \tag{35}$$

because

$$\begin{aligned} \boldsymbol{\nabla}_K\langle\phi_i|\phi_j\rangle &= \boldsymbol{\nabla}_K\delta_{ij} = 0 && (36)\\ &= \langle\boldsymbol{\nabla}_K\phi_i|\phi_j\rangle + \langle\phi_i|\boldsymbol{\nabla}_K\phi_j\rangle = \mathbf{d}_{ji}^* + \mathbf{d}_{ij} \quad . && (37) \end{aligned}$$

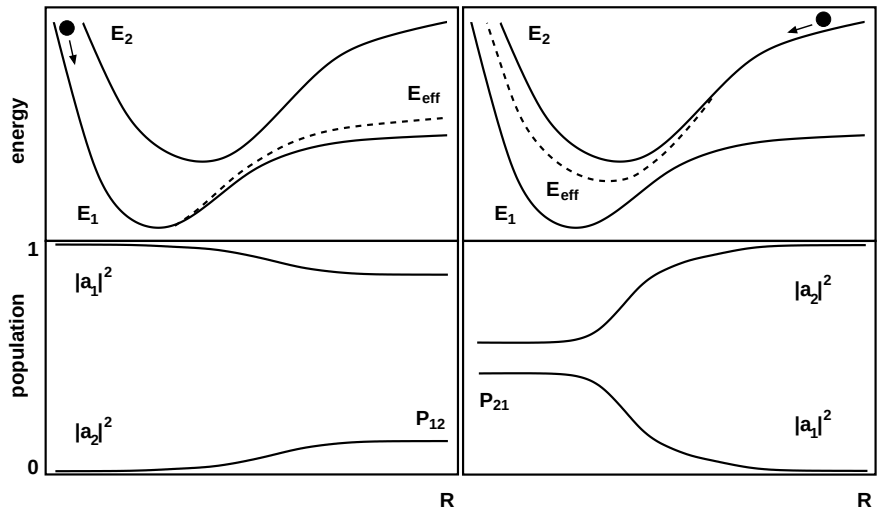

Figure 3. Top left: forward path effective potential, $E_{\rm eff}$, for two weakly coupled adiabatic PES, E_1 and E_2. Bottom left: state occupations for a system initially prepared in state 1. The final value of $|a_2|^2$ is equal to the transition probability P_{12}. Top right: backward path effective potential, $E_{\rm eff}$, for two weakly coupled adiabatic PES, E_1 and E_2. Bottom left: state occupations for a system initially prepared in state 2. The final value of $|a_1|^2$ is equal to the transition probability P_{21}.

Equating the rhss (right hand sides) of Eqs. (30) and (32) one obtains after rearranging,

$$\langle\phi_i|\boldsymbol{\nabla}_K\mathcal{H}_{\rm el}|\phi_j\rangle = \boldsymbol{\nabla}_K E_i\delta_{ij} - (E_j - E_i)\mathbf{d}_{ji} \quad . \tag{38}$$

The nuclear forces (Eq. (29)) are thus given by

$$\mathbf{F}_K = -\sum_i |a_i|^2\boldsymbol{\nabla}_K E_i + \sum_{i,j} a_i^* a_j (E_j - E_i)\mathbf{d}_{ji} \quad . \tag{39}$$

Eq. (39) illustrates the two contributions to the nuclear forces; the first term is simply the population-weighted average force over the adiabatic states, while the second term takes into account nonadiabatic changes of the adiabatic state occupations. We would like to point out here that the nonadiabatic contributions to the nuclear forces are in the direction of the nonadiabatic coupling vectors $\mathbf{d}_{ji}$.

The Ehrenfest method has been applied with great success to a number of chemical problems including energy transfer at metal surfaces[19]. However, due to its mean-field character the method has some serious limitations. A system that was initially prepared in a pure adiabatic state will be in a mixed state when leaving the region of strong nonadiabatic coupling. In general, the pure adiabatic character of the wavefunction cannot be recovered even in the asymptotic regions of configuration space. In cases where the differences in the adiabatic potential energy landscapes are pronounced, it is clear that an average potential will be unable to describe all reaction channels adequately. In particular, if one is interested in a reaction branch whose occupation number is very small, the average path is likely to diverge from the true trajectory. Furthermore, the total wavefunction may contain significant contributions from adiabatic states that are energetically inaccessible (see Figure 2).

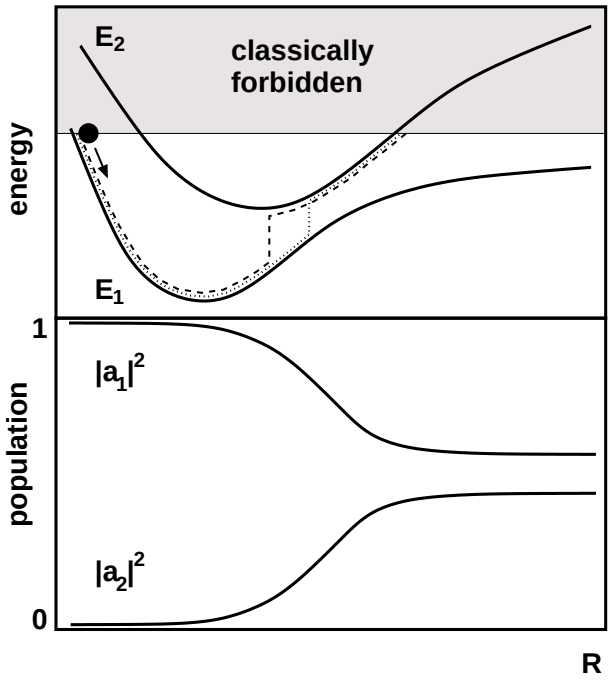

Figure 4. Top: avoided crossing between two adiabatic PES, E_1 and E_2, and two typical forward surface hopping trajectories. Nonadiabatic transitions are most likely to occur in the coupling region. Bottom: corresponding adiabatic state populations $|a_1|^2$ and $|a_1|^2$. The system is prepared to be in state 1 initially with zero kinetic energy. Upon entering the coupling region state 2 is increasingly populated.

Figure 3 illustrates another severe drawback of the mean-field approach. The principle of microscopic reversibility demands that the forward path probability, $P_{12}^{\rm for} = |a_2^{\rm final}|^2$ for a system that was initially prepared in state 1 to end up in state 2 must be equal to the backward path probability, $P_{21}^{\rm back} = |a_1^{\rm final}|^2$ for a system that was initially prepared in state 2 to end up in state 1. One can easily think of situations, like the one depicted in Figure 3, for which the effective potentials for the forward and backward paths are very different, resulting also in different populations, $|a_i|^2$. The Ehrenfest method, therefore, violates microscopic reversibility.

It should be noted that the expansion of the total wavefunction in terms of (adiabatic) basis functions (Eq. (18)) is not a necessary requirement for the Ehrenfest method; the wavepacket Φ can be propagated numerically using Eq. (17). However, projection of Φ onto the adiabatic states facilitates interpretation. Knowledge of the expansion coefficients, a_i, is also the key to refinements of the method such as the surface hopping technique.

4.2 Surface Hopping

We have argued above that after exiting a well localised nonadiabatic coupling region it is unphysical for nuclear motion to be governed by a mixture of adiabatic states. Rather it would be desirable that in asymptotic regions the system evolves on a pure adiabatic PES.

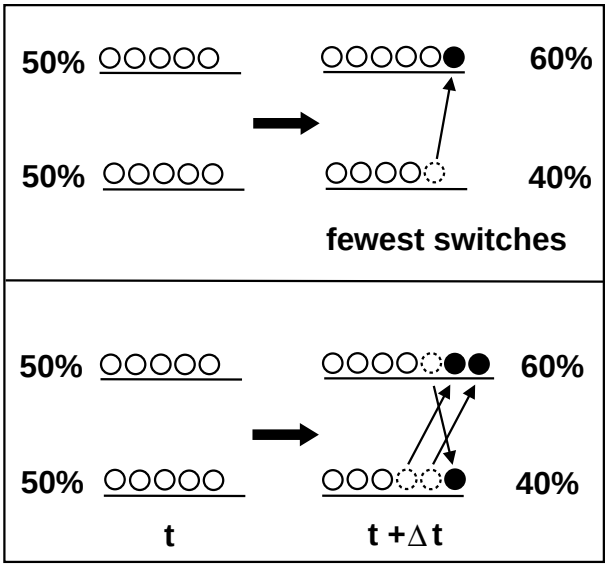

Figure 5. A two-state system with each state being equally (50%) populated at time t. At time $t + \Delta t$ the lower and the upper state are populated by 40 % and 60 % of ensemble members, respectively. The top panel shows how this distribution can be achieved with the minimum number of transitions, whereas the bottom panel shows *one* alternative route involving a larger number of transitions.

This idea is fundamental to the surface hopping approach. Instead of calculating the 'best' (i.e., state-averaged) path like in the Ehrenfest method, the surface hopping technique involves an ensemble of trajectories. At any moment in time, the system is propagated on some pure adiabatic state i, which is selected according to its state population $|a_i|^2$. Changing adiabatic state occupations can thus result in nonadiabatic transitions between different adiabatic PESs (see Figure 4). The ensemble averaged number of trajectories evolving on adiabatic state i at any time is equal to its occupation number $|a_i|^2$.

In the original formulation of the surface hopping method by Tully and Preston[11], switches between adiabatic states were allowed only at certain locations defined prior to the simulation. Tully[12] later generalized the method in such a way that nonadiabatic transitions can occur at any point in configuration space. At the same time, an algorithm — the so-called fewest switches criterion — was proposed which minimises the number of surface hops per trajectory whilst guaranteeing the correct ensemble averaged state populations at all times. The latter is important because excessive surface switching effectively results in weighted averaging over the adiabatic states much like in the case of the Ehrenfest method.

We shall now derive the fewest switches criterion. Out of a total of N trajectories, N_i will be in state i at time t,

$$N_i(t) = \rho_{ii}(t)N \quad . \tag{40}$$

Here we have introduced the density matrix notation

$$\rho_{ij}(t) = a_i^*(t)a_j(t) \quad . \tag{41}$$

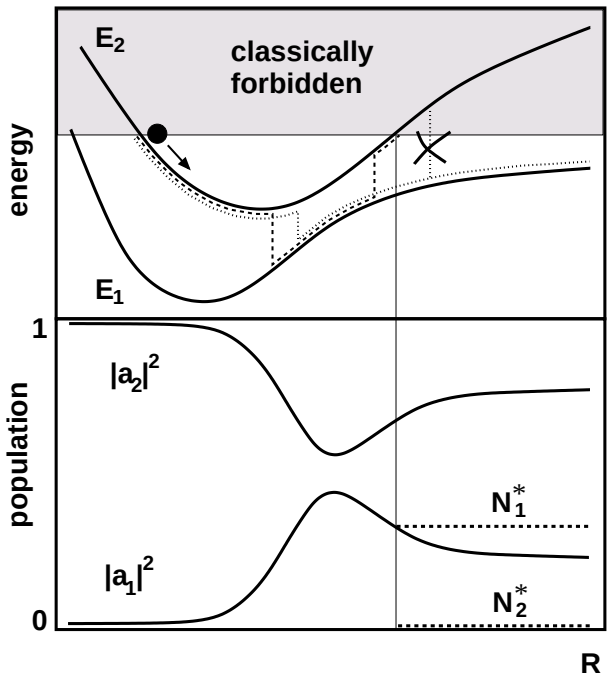

Figure 6. Top: avoided crossing between two adiabatic PES, E_1 and E_2, and two typical forward surface hopping trajectories. Nonadiabatic transitions are most likely to occur in the coupling region. The cross indicates a classically forbidden transition; no switch is carried out in this case. Bottom: corresponding adiabatic state populations $|a_1|^2$ and $|a_1|^2$. The system is prepared in state 2 initially with zero kinetic energy. Upon entering the coupling region state 1 is increasingly populated. Upon exiting the coupling region, state population 1 decreases. For configurations $\mathbf{R}$ for which E_2 is in the classically forbidden region, the percentages of trajectories in state i, N_i^*, are unequal to $|a_i|^2$; N_2^* is zero whereas N_1^* remains constant.

At a later time $t' = t + \delta t$ the new occupation numbers are

$$N_i(t') = \rho_{ii}(t')N \tag{42}$$

Let us suppose that $N_i(t') < N_i(t)$ or $\delta N = N_i(t) - N_i(t') > 0$. Then the minimum number of transitions required to go from $N_i(t)$ to $N_i(t')$ is δN hops from state i to any other state and zero hops from any other state to state i (see Figure 5). The probability $P_i(t, \delta t)$ for a transition out of state i to any other state during the time interval $[t, t + \delta t]$ is then given by

$$P_i(t, \delta t) = \frac{\delta N}{N_i} = \frac{\rho_{ii}(t) - \rho_{ii}(t')}{\rho_{ii}} \approx -\frac{\dot{\rho_{ii}}\delta t}{\rho_{ii}} \quad , \tag{43}$$

where we have used

$$\dot{\rho_{ii}} \approx \frac{\rho_{ii}(t') - \rho_{ii}(t)}{\delta t} \quad . \tag{44}$$

The lhs of Eq. (44) can be written as

$$\dot{\rho_{ii}} = \frac{\mathrm{d}}{\mathrm{d}t}(a_i^* a_i) = \dot{a_i^*} a_i + a_i^* \dot{a_i} = (a_i^* \dot{a_i})^* + a_i^* \dot{a_i} = 2\Re(a_i^* \dot{a_i}) \quad . \tag{45}$$

Inserting Eq. (19) into Eq. (45) we obtain

$$\dot{\rho_{ii}} = -2\Re\left(\sum_j \rho_{ij} C_{ij} e^{-\frac{i}{\hbar}\int (E_j - E_i)\mathrm{d}t}\right) \quad . \tag{46}$$

Substituting expression (46) into Eq. (43) the probability P_i can be rewritten as follows

$$P_i(t, \delta t) = \frac{2\Re\left(\sum_j \rho_{ij} C_{ij} e^{-\frac{i}{\hbar}\int (E_j - E_i)\mathrm{d}t}\right)\delta t}{\rho_{ii}} \quad . \tag{47}$$

Since the probability, P_i, for a switch from state i to any other state must be the sum over all states of the probabilities, P_{ij}, for a transition from state i to a specific state j,

$$P_i(t, \delta t) = \sum_j P_{ij}(t, \delta t) \quad , \tag{48}$$

it follows from Eq. (47) that

$$P_{ij}(t, \delta t) = \frac{2\Re\left(\rho_{ij} C_{ij} e^{-\frac{i}{\hbar}\int (E_j - E_i)\mathrm{d}t}\right)\delta t}{\rho_{ii}} \quad . \tag{49}$$

A transition from state i to state k is now invoked if

$$P_i^{(k)} < \zeta < P_i^{(k+1)} \quad , \tag{50}$$

where ζ ($0 \leq \zeta \leq 1$) is a uniform random number and $P_i^{(k)}$ is the sum of the transition probabilities for the first k states,

$$P_i^{(k)} = \sum_j^k P_{ij} \quad . \tag{51}$$

In order to conserve total energy after a surface hop has been carried out, the atomic velocities have to be rescaled. The usual procedure is to adjust only the velocity components in the direction of the nonadiabatic coupling vector $d_{ik}(\mathbf{R})$ (Eq. (33))[12]. We can qualitatively justify this practice by our earlier observation that the nonadiabatic contribution to the Ehrenfest forces also are in the direction of the nonadiabatic coupling vector $d_{ik}(\mathbf{R})$ (see Eq. (39)). Certainly, such discontinuities in nuclear velocities must be regarded as a flaw of the surface hopping approach. In most physical scenarios, however, nonadiabatic surface switches take place only at relatively small potential energy separations so that the necessary adjustment to the nuclear velocities is reasonably small. Nevertheless, a severe limitation of the method is presented by its inability to properly deal with situations in which the amount of kinetic energy is insufficient to compensate for the difference in potential energy (so-called classically forbidden transitions). Tully's original suggestion not to carry out a surface hop while retaining the nuclear velocities in such cases has been demonstrated[20] to be more accurate than later proposals to reverse the velocity components in the direction of the nonadiabatic coupling vector $d_{ik}(\mathbf{R})$[21,22]. The example presented in Figure 6 illuminates how classically forbidden transitions cause divergence between the target occupation numbers, $|a_i|^2$, and the actual percentages of trajectories

evolving in state i, N_i^*.

It should be noted that surface hopping exhibits a large degree of electronic coherence through continuous integration of Eqs. (19) along the entire trajectory. On the one hand, this enables the method to reproduce quantum interference effects[12] such as Stueckelberg oscillations[15]. On the other hand, due to treating nuclei classically, dephasing of the electronic degrees of freedom may be too slow, a shortcoming shared by the surface hopping and the Ehrenfest method alike. A number of semiclassical approaches incorporating decoherence have, therefore, been proposed[23–29]. Some of these alternative methods attempt to combine the advantages of surface hopping (mainly, pure adiabatic states in asymptotic regions) with those of the mean-field method (no discontinuities in potential energy, no disallowed transitions) by employing an effective potential whilst enforcing gradual demixing of the total wavefunction away from the coupling regions[27–29].

4.3 Car-Parrinello Surface Hopping

So far we have assumed that a number of adiabatic potential energy surfaces (at least two) have been obtained by solving the time-independent Schrödinger equation (10) in some unspecified manner. Instead of precalculating the entire PESs, it is advantageous to compute the electronic energies and nuclear gradients "on the fly" as the system is propagated along the trajectory. A popular method in this context has been the Diatomics-in-Molecules (DIM)[30–42] method which cheaply provides the required electronic eigenvalues and atomic forces for a multitude of molecular valence states simultaneously through diagonalisation of the Hamiltonian matrix. However, although the DIM method works remarkably well for some simple systems such as cationic rare-gas clusters[43–46], it is not generally applicable to more complex systems.

For ground state calculations, density functional theory[47–49] based *ab initio* MD in the spirit of Car and Parrinello[50] has become the method of choice to study large molecules and condensed phase systems. Recently, Car-Parrinello simulations have become possible also in the first excited singlet state using a restricted open-shell Kohn-Sham (ROKS) approach[51]. We summarize here a recently developed Tully-style[12] trajectory surface hopping method coupling nonadiabatically the S_0 ground state and the S_1 excited state accessible within the Car-Parrinello framework[52–54]. This approach has been applied to a variety of problems including photoisomerisation[52], excited state intramolecular proton transfer[55], and the photochemistry of nucleobases[56,57,55,58].

4.3.1 Restricted Open-Shell Kohn-Sham Method

Let us first take a brief look at the ROKS method for the S_1 state. Starting from a closed-shell ground state, S_0, consider an excitation of an electron out of the HOMO into the LUMO. The resulting two unpaired spins can be arranged in four different ways, as illustrated in Figure 7, parallel spins forming triplet determinants and antiparallel spins being equal mixtures of singlet and triplet determinants. The S_1 singlet wavefunction, ϕ_1, is constructed as

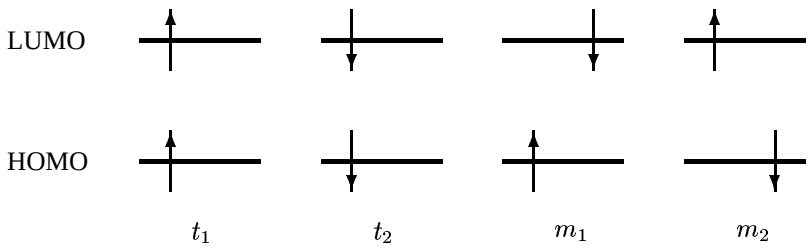

Figure 7. Four possible spin configurations upon excitation of one electron out of the highest occupied molecular orbital (HOMO) to the lowest unoccupied molecular orbital (LUMO). The two parallel spin configurations, t_1 and t_2 form triplet determinants, while the two antiparallel configurations, m_1 and m_2 form mixed determinants with equal singlet and triplet contributions.

$$\begin{aligned}\phi_1 &= \frac{1}{\sqrt{2}}\{|m_1\rangle + |m_2\rangle\} \\ &= \frac{1}{\sqrt{2}}\Big\{|\varphi_1^{(1)}\bar{\varphi}_1^{(1)}\varphi_2^{(1)}\bar{\varphi}_2^{(1)}\cdots\varphi_l^{(1)}\bar{\varphi}_{l+1}^{(1)}\rangle \\ &\qquad + |\varphi_1^{(1)}\bar{\varphi}_1^{(1)}\varphi_2^{(1)}\bar{\varphi}_2^{(1)}\cdots\varphi_{l+1}^{(1)}\bar{\varphi}_l^{(1)}\rangle\Big\} \quad ,\end{aligned} \tag{52}$$

where the "ket" notation signifies Slater determinants made up of Kohn-Sham orbitals, $\varphi_i^{(1)}$ (spin up) and $\bar{\varphi}_i^{(1)}$ (spin down); $l = \frac{n}{2}$ is half the number of electrons.
It has been shown by Ziegler et al.[59] that the S_1 energy, $E(S_1)$, can be written as the difference between twice the energy of the mixed determinant, $E(m)$, and the energy of the triplet determinant, $E(t)$,

$$E(S_1) = 2E(m) - E(t) \quad . \tag{53}$$

Within the ROKS scheme, a *single* set of orbitals $\{\varphi_i^{(1)}\}$ is determined that minimises the energy functional,

$$E[\{\varphi_i^{(1)}\}] = 2\langle m|\mathcal{H}^{\mathrm{KS}}|m\rangle - \langle t|\mathcal{H}^{\mathrm{KS}}|t\rangle - \sum_{i,j=1}^{l+1}\lambda_{ij}\Big\{\langle\varphi_i^{(1)}|\varphi_j^{(1)}\rangle - \delta_{ij}\Big\} \quad , \tag{54}$$

where $\mathcal{H}^{\mathrm{KS}}$ is the Kohn-Sham Hamiltonian[49] and the λ_{ij} are Lagrange multipliers taking care of the orthonormality of the orbitals.

Due to this optimisation the entire set of orbitals $\{\varphi_i^{(1)}\}$ will, in general, differ from the set of orbitals $\{\varphi_i^{(0)}\}$ that define the ground state wavefunction, ϕ_0,

$$\phi_0 = |\varphi_1^{(0)}\bar{\varphi}_1^{(0)}\varphi_2^{(0)}\bar{\varphi}_2^{(0)}\cdots\varphi_l^{(0)}\bar{\varphi}_l^{(0)}\rangle \quad . \tag{55}$$

As a consequence the two state functions, ϕ_0 and ϕ_1, are nonorthogonal giving rise to the overlap matrix elements, S_{ij},

$$S_{01} = S_{10} \equiv S \, , \quad S_{ii} = 1 \quad . \tag{56}$$

4.3.2 S_0–S_1 Surface Hopping

Inserting ansatz (Eq. (18)) using the above basis functions, ϕ_0 and ϕ_1, into Eq. (17) and replacing $\mathcal{H}_{\rm el}$ with $\mathcal{H}^{\rm KS}$ we obtain after integration over the electronic coordinates following multiplication by ϕ_i^* from the left

$$\sum_j a_j p_j (H_{ij} - E_j S_{ij}) = i\hbar \left\{ \sum_j \dot{a}_j p_j S_{ij} + \sum_j a_j p_j C_{ij} \right\} \quad , \tag{57}$$

where the Hamiltonian matrix elements are given by

$$H_{ii} = \langle \Phi_i | \mathcal{H}^{\rm KS} | \Phi_i \rangle = E_i \quad , \tag{58}$$

$$H_{01} = H_{10} = E_0 S \quad , \tag{59}$$

and the phase factor has been abbreviated as

$$p_j \equiv e^{-\frac{i}{\hbar}\int E_j dt} \quad . \tag{60}$$

We should stress here that the discrepancy between Eqs. (57) and (19) arises purely because ϕ_1 is *not* an eigenfunction of $\mathcal{H}^{\rm KS}$.
For $i = 0$, Eq. (57) thus becomes

$$a_1 p_1 S(E_0 - E_1) = i\hbar \left\{ \dot{a}_0 p_0 + \dot{a}_1 p_1 S + a_1 p_1 C_{01} \right\} \quad , \tag{61}$$

and for $i = 1$

$$0 = \dot{a}_0 p_0 S + \dot{a}_1 p_1 + a_0 p_0 C_{10} \quad . \tag{62}$$

Solving equations (61) and (62) for $\dot{a}_0$ and $\dot{a}_1$ one finds

$$\dot{a}_0 = \frac{1}{S^2 - 1} \left[i a_1 \frac{p_1}{p_0} S(E_0 - E_1) + a_1 C_{01} \frac{p_1}{p_0} - a_0 C_{10} S \right] \quad , \tag{63}$$

$$\dot{a}_1 = \frac{1}{S^2 - 1} \left[a_0 C_{10} \frac{p_0}{p_1} - a_1 C_{01} S - i a_1 S^2 (E_0 - E_1) \right] \quad . \tag{64}$$

We integrate these two coupled differential equations numerically using a fourth order Runge-Kutta scheme[60]. It is computationally attractive to work with the nonadiabatic coupling elements, C_{ij} (Eq. (20), instead of the nonadiabatic coupling vectors, $\mathbf{d}_{ji}$ (Eq. (33), since the orbital velocities are readily available within the Car-Parrinello method.

If both electronic state functions were eigenfunctions of the Kohn-Sham Hamiltonian, $|a_0|^2$ and $|a_1|^2$ would be their respective occupation numbers. A look at the normalisation integral of the total wavefunction Φ,

$$\langle \Phi | \Phi \rangle = |a_0|^2 + |a_1|^2 + 2S\,\Re\left(a_0^* a_1 \frac{p_1}{p_0} \right) \equiv 1 \quad , \tag{65}$$

shows that the definition of state populations in this basis is ambiguous. We therefore expand the total wavefunction Φ in terms of an orthonormal set of auxiliary wavefunctions, ϕ_0' and ϕ_1':

$$\Phi = d_0 \phi_0' + d_1 \phi_1' = b_0 \phi_0 + b_1 \phi_1 \quad , \tag{66}$$

where

$$\langle \phi_i' | \phi_j' \rangle = \delta_{ij} \tag{67}$$

and

$$b_j = a_j p_j \quad . \tag{68}$$

Since Φ is normalised, the squares of our new expansion coefficients add up to unity and thus have the meaning of state populations in the orthogonal basis:

$$|d_0|^2 + |d_1|^2 = 1 \quad . \tag{69}$$

The orthonormal wavefunctions ϕ_0' and ϕ_1' can be expressed in terms of ϕ_0 and ϕ_1 as

$$\phi_0' = c_{00}\phi_0 + c_{10}\phi_1 \quad , \tag{70}$$

$$\phi_1' = c_{01}\phi_0 + c_{11}\phi_1 \quad , \tag{71}$$

$\mathbf{c}_0 = \begin{pmatrix} c_{00} \\ c_{10} \end{pmatrix}$ and $\mathbf{c}_1 = \begin{pmatrix} c_{01} \\ c_{11} \end{pmatrix}$ being solutions of the eigenvalue problem

$$\mathbf{HC} = \mathbf{SCE} \quad . \tag{72}$$

Using the Hamiltonian matrix elements of Eqs. (58) and (59) and the overlap matrix of Eq. (56), one obtains the eigenvalues

$$e_0 = E_0 \tag{73}$$

and

$$e_1 = \frac{E_1 - S^2 E_0}{1 - S^2} \quad (> E_1, \text{ if } E_0 < E_1) \quad . \tag{74}$$

The corresponding eigenvectors are

$$\mathbf{c}_0 = \begin{pmatrix} 1 \\ 0 \end{pmatrix} \tag{75}$$

and

$$\mathbf{c}_1 = \begin{pmatrix} -S \\ 1 \end{pmatrix} \tag{76}$$

leading to the orthonormal wavefunctions

$$\phi_0' = \phi_0 \quad , \tag{77}$$

$$\phi_1' = \frac{1}{\sqrt{1 - S^2}} [-S\phi_0 + \phi_1] \quad . \tag{78}$$

Inserting Eqs. (77) and (78) into Eq. (66) we determine the expansion coefficients to be

$$d_0 = b_0 + b_1 S \tag{79}$$

$$d_1 = b_1 \sqrt{1 - S^2} \quad . \tag{80}$$

The state occupation numbers are thus

$$|d_0|^2 = |b_0|^2 + S^2|b_1|^2 + 2S\,\Re(b_0^* b_1) \quad , \tag{81}$$

$$|d_1|^2 = (1 - S^2)|b_1|^2 \tag{82}$$

or alternatively

$$|d_0|^2 = |a_0|^2 + S^2|a_1|^2 + 2S\,\Re\left(a_0^* a_1 \frac{p_1}{p_0}\right) \tag{83}$$

$$|d_1|^2 = (1 - S^2)|a_1|^2 \quad . \tag{84}$$

We are now in a position to apply Tully's fewest switches criterion (Eq. (49)) using the coefficients d_i to construct the density matrix (Eq. (41)).

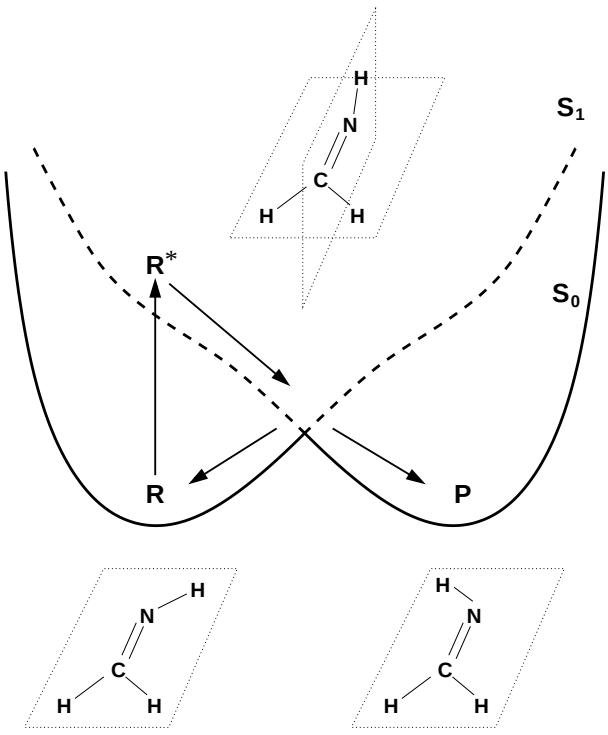

Figure 8. Schematic view of the photoreaction pathways of formaldimine. S_0 and S_1 energy curves are plotted against the reaction coordinate whose main contributor is the NH twist angle. The reactant R is vertically excited from the ground state into the S_1 state to form R*. The system then falls into a conical intersection where relaxation to the ground state occurs. The reaction can proceed to either of the equivalent isomers, R and P. Formation of the photoproduct P corresponds to photoisomerisation.

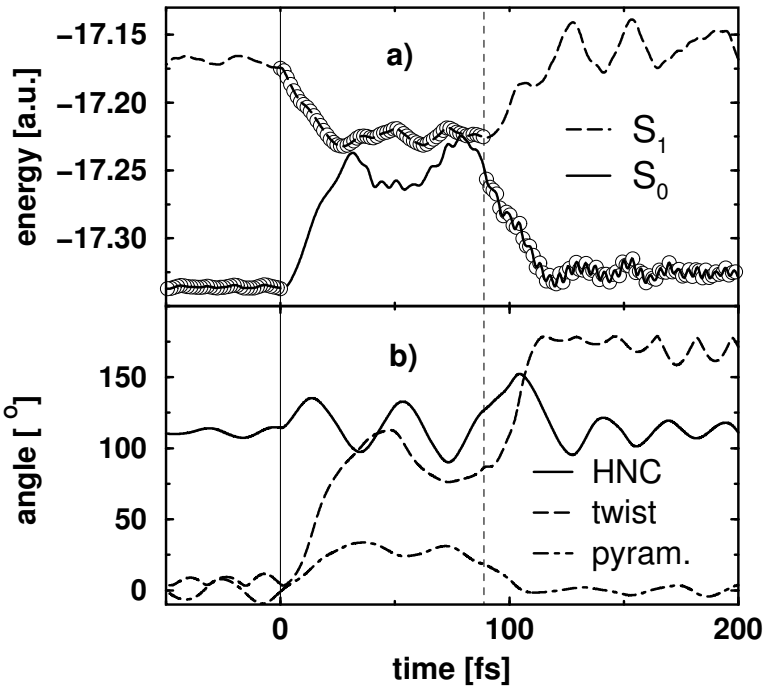

Figure 9. a) Time evolution of S_0 and S_1 energies following photoexcitation in the case of a successful R $\rightarrow$ P reaction. The solid and dashed vertical lines indicate the moment of the photoexcitation and the nonadiabatic transition to the ground state, respectively. The open circles denote the PES on which the nuclei are being propagated. b) Corresponding time evolution of the pyramidalisation, HNC and the HN twist angles. The HN bond is seen to flip from 0° to 180° resulting in the photoproduct. For HNC angles around 106.5° at orthogonal twist geometry, the energy gap is seen to be minimal.

4.3.3 Example: Photoisomerisation of Formaldimine

Figure 8 shows a schematic view of the photoreaction pathways of formaldimine. The reactant, R, is excited vertically from the ground state minimum into the S_1 state to form R*. Subsequently, the system moves along the reaction coordinate, which predominantly involves an out-of-plane twist of the NH bond, into a conical intersection located at orthogonal twist geometry. In this region of strong nonadiabatic coupling a transition to the ground state occurs leading either to the photoisomerisation product, P, or back to the reactant R. As starting configurations for our nonadiabatic CP–MD calculations, we have picked 100 initial conditions at random from a standard ground state run at 300 K, in order to sample the canonical ensemble. For each of the two possible outcomes, i.e. R $\rightarrow$ P and R $\rightarrow$ R, a typical trajectory is analysed in Figures. 9 and 10[61]. Figure 9a shows the evolution of the S_0 and S_1 energies as a function of time for a reactive trajectory leading to the photoproduct P. A photochemical laser excitation of the system is mimicked by vertical $S_0 \rightarrow S_1$ excitation at $t = 0$ (see circles in Figure 9a). The system is seen to quickly move down into the S_1 potential well dramatically reducing the energy gap to the ground state. As illustrated by Figure 9b, the main contribution to the S_1 energy reduction

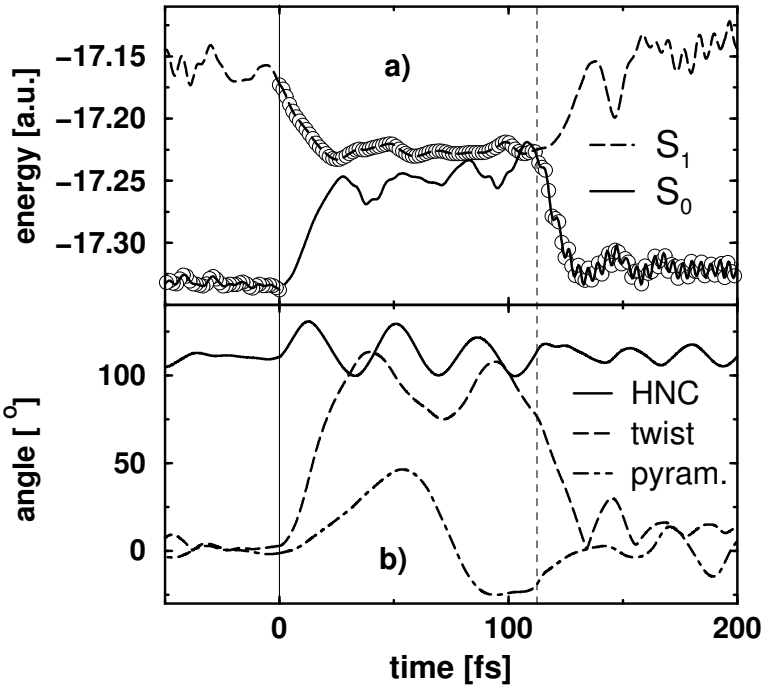

Figure 10. a) Time evolution of S_0 and S_1 energies following photoexcitation for a non-reactive R $\rightarrow$ R event (all symbols as in Figure 9.) b) Corresponding time evolution of the pyramidalisation, HNC and the HN twist angles. The HN bond is seen to orthogonalise initially and later flip back to $0°$.

is due to the NH twist angle changing from near planarity ($0°$) to orthogonality ($90°$). Near the minimum of the S_1 PES, where the nonadiabatic coupling is strongest, a nonadiabatic transition to the S_0 state occurs leading to rapid widening of the energy gap accompanied by a change in the twist angle from around $90°$ to near $180°$. This behaviour is in accord with static MRCI predictions[52,62]. Additional insight can be gained by analysing the role of the HNC and pyramidalisation angles. It becomes clear that pyramidalisation is pre-requisite for the two surfaces to cross. Similarly, small HNC angles minimise the energy gap, maximising the nonadiabatic transition probability. In the case of the non-reactive R $\rightarrow$ R event (Figure 10), the situation is initially very similar with the exception that the nonadiabatic surface hop occurs one HNC vibrational period later. Furthermore, the NH twist angle relaxes back to near $0°$ after initial orthogonalisation, signifying an unsuccessful photoisomerisation attempt. The two surfaces are seen to cross near orthogonal twist geometry with the HNC and pyramidalisation angles being close to a minimum and maximum, respectively.

It is possible, in principle, to determine the quantum yield of photoisomerisation by averaging over an ensemble of surface hopping trajectories. Since this would be beyond the scope of this article, we can only state here our non-converged result of 70 %.

Acknowledgements

I should like to thank Prof. D. Marx for his support.

References

1. V. Bonačić-Koutecký and R. Mitrić. *Chem. Rev.*, 105:11, 2005.
2. M. D. Hack and D. G. Truhlar. *J. Phys. Chem.* A, 104:7917, 2000.
3. M. P. Allen and D. J. Tildesley. *Computer Simulation of Liquids*. Clarendon Press, Oxford, 1987.
4. D. Frenkel and B. Smit. *Understanding Molecular Simulation. From Algorithms to Applications*. Academic Press, Boston, 1996.
5. P. Ehrenfest. *Z. Phys.*, 45:455, 1927.
6. H.-D. Meyer and W. H. Miller. *J. Chem. Phys.*, 70:3214, 1979.
7. D. A. Micha. *J. Chem. Phys.*, 78:7138, 1983.
8. J. C. Tully. In B. J. Berne, G. Ciccotti, and D. F. Coker, editors, *Classical and Quantum Dynamics in Condensed Phase Simulations*. World Scientific, Singapore, 1998.
9. J. C. Tully. In D. L. Thompson, editor, *Modern Methods for Multidimensional Dynamics Computations in Chemistry*. World Scientific, Singapore, 1998.
10. X. Li, J. C. Tully, H. B. Schlegel, and M. J. Frisch. *J. Chem. Phys.*, 123:084106, 2005.
11. J. C. Tully and R. K. Preston. *J. Chem. Phys.*, 55:562, 1971.
12. J. C. Tully. *J. Chem. Phys.*, 93:1061, 1990.
13. N. C. Blair and D. G. Truhlar. *J. Chem. Phys.*, 79:1334, 1983.
14. P. J. Kuntz. *J. Chem. Phys.*, 95:141, 1991.
15. E. E. Nikitin. In H. Hartmann, editor, *Chemische Elementarprozesse*. Springer, Berlin, 1968.
16. E. E. Nikitin and L. Zülicke. *Theory of Chemical Elementary Processes*. Springer, Berlin, 1978.
17. L. Salem. *Electrons in Chemical Reactions: First Principles*. Wiley, New York, 1982.
18. L. Salem, C. Leforestier, G. Segal, and R. Wetmore. *J. Am. Chem. Soc.*, 97:479, 1975.
19. J. C. Tully, M. Gomez, and M. Head-Gordon. *J. Vac. Sci. Technol.*, A11:1914, 1993.
20. U. Müller and G. Stock. *J. Chem. Phys.*, 107:6230, 1997.
21. S. Hammes-Schiffer and J. C. Tully. *J. Chem. Phys.*, 101:4657, 1994.
22. D. F. Coker and L. Xiao. *J. Chem. Phys.*, 102:496, 1995.
23. F. Webster, P. J. Rossky, and R. A. Friesner. *Comp. Phys. Comm.*, 63:494, 1991.
24. F. J. Webster, J. Schnitker, M. S. Friedrichs, R. A. Friesner, and P. J. Rossky. *Phys. Rev. Lett.*, 66:3172, 1991.
25. E. R. Bittner and P. J. Rossky. *J. Chem. Phys.*, 103:8130, 1995.
26. E. R. Bittner and P. J. Rossky. *J. Chem. Phys.*, 107:8611, 1997.
27. M. D. Hack and D. G. Truhlar. *J. Chem. Phys.*, 114:2894, 2001.
28. M. D. Hack and D. G. Truhlar. *J. Chem. Phys.*, 114:9305, 2001.

29. Y. L. Volobuev, M. D. Hack, M. S. Topaler, and D. G. Truhlar. *J. Chem. Phys.*, 112:9716, 2000.
30. F. O. Ellison. *J. Am. Chem. Soc.*, 85:3540, 1963.
31. J. C. Tully. *J. Chem. Phys.*, 59:5122, 1973.
32. J. C. Tully. *J. Chem. Phys.*, 58:1396, 1973.
33. J. C. Tully. *J. Chem. Phys.*, 64:3182, 1976.
34. J. C. Tully and C. M. Truesdale. *J. Chem. Phys.*, 65:1002, 1976.
35. P. J. Kuntz and A. C. Roach. *J. Chem. Soc. Faraday Trans.*, 68:259, 1971.
36. E. Steiner, P. R. Certain, and P. J. Kuntz. *J. Chem. Phys.*, 59:47, 1973.
37. P. J. Kuntz. *J. Phys. B*, 19:1731, 1986.
38. A. C. Roach and P. J. Kuntz. *J. Chem. Phys.*, 84:822, 1986.
39. J. C. Tully. In G. A. Segal, editor, *Modern Theoretical Chemistry*, Vol. 7A. Plenum Press, New York, 1977.
40. P. J. Kuntz. In R. B. Bernstein, editor, *Atom-Molecule Collision Theory*. Plenum Press, New York, 1979.
41. P. J. Kuntz. In M. Baer, editor, *Theory of Chemical Reaction Dynamics*, Vol. 1. Chemical Rubber, Boca Raton, 1985.
42. P. J. Kuntz. In Z. B. Maksic, editor, *Theoretical Models of Chemical Bonding*, Part 2. Springer, Berlin, 1990.
43. N. L. Doltsinis and P. J. Knowles. *Chem. Phys. Let.*, 325:648, 2000.
44. N. L. Doltsinis. *Mol. Phys.*, 97, 1999.
45. N. L. Doltsinis and P. J. Knowles. *Chem. Phys. Lett.*, 301:241, 1999.
46. N. L. Doltsinis, P. J. Knowles, and F. Y. Naumkin. *Mol. Phys.*, 96:749, 1999.
47. R. G. Parr and W. Yang. *Density Functional Theory of Atoms and Molecules*. Oxford University Press, Oxford, 1989.
48. P. Hohenberg and W. Kohn. *Phys. Rev.* B, 136:864, 1964.
49. W. Kohn and L. J. Sham. *Phys. Rev.* A, 140:1133, 1965.
50. R. Car and M. Parrinello. *Phys. Rev. Lett.*, 55:2471, 1985.
51. I. Frank, J. Hutter, D. Marx, and M. Parrinello. *J. Chem. Phys.*, 108:4060, 1998.
52. N. L. Doltsinis and D. Marx. *Phys. Rev. Lett.*, 88:166402, 2002.
53. N. L. Doltsinis. In J. Grotendorst, D. Marx, and A. Muramatsu, editors, *Quantum Simulations of Complex Many-Body Systems: From Theory to Algorithms*. NIC, FZ Jülich, 2002.
`www.fz-juelich.de/nic-series/volume10/doltsinis.pdf`.
54. N. L. Doltsinis and D. Marx. *J. Theor. Comp. Chem.*, 1:319–349, 2002.
55. N. L. Doltsinis. *Mol. Phys.*, 102:499, 2004.
56. H. Langer and N. L. Doltsinis. *Phys. Chem. Chem. Phys.*, 5:4516, 2003.
57. H. Langer and N. L. Doltsinis. *Phys. Chem. Chem. Phys.*, 6:2742, 2004.
58. H. Langer, N. L. Doltsinis, and D. Marx. *ChemPhysChem*, 6:1734, 2005.
59. T. Ziegler, A. Rauk, and E. J. Baerends. *Theor. Chim. Acta*, 43:261, 1977.
60. W. H. Press, S. A. Teukolsky, W. T. Vetterling, and B. P. Flannery. *Numerical Recipes in Fortran 77*, volume 1. Cambridge University Press, 1999.
61. For a graphical animation see
`www.theochem.ruhr-uni-bochum.de/go/surfhop.html`.
62. V. Bonačić-Koutecký and Josef Michl. *Theor. Chim. Acta*, 68:45, 1985.